Received: 23 March 2016 | Revised: 4 April 2017

DOI: 10.1002/jae.2585

RESEARCH ARTICLE

WILEY Journal of APPLIED ECONOMETRICS

Estimating global bank network connectedness

Mert Demirer[1] | Francis X. Diebold[2] | Laura Liu[2] | Kamil Yilmaz[3]

[1]MIT, Cambridge, MA 02139, USA

[2]University of Pennsylvania, Philadelphia, PA 19104, USA

[3]Koç University, Istanbul, Turkey

Correspondence
Kamil Yilmaz, Koç University, Rumelifeneri Yolu, Sariyer, Istanbul 34450 Turkey.
Email: kyilmaz@ku.edu.tr

Summary

We use LASSO methods to shrink, select, and estimate the high-dimensional network linking the publicly traded subset of the world's top 150 banks, 2003–2014. We characterize static network connectedness using full-sample estimation and dynamic network connectedness using rolling-window estimation. Statically, we find that global bank equity connectedness has a strong geographic component, whereas country sovereign bond connectedness does not. Dynamically, we find that equity connectedness increases during crises, with clear peaks during the Great Financial Crisis and each wave of the subsequent European Debt Crisis, and with movements coming mostly from changes in cross-country as opposed to within-country bank linkages.

1 | INTRODUCTION

Connectedness is central to modern financial risk measurement and management. It features prominently in key aspects of market risk (return connectedness and portfolio concentration), credit risk (default connectedness), counter-party and gridlock risk (bilateral and multilateral contractual connectedness), and, not least, systemic risk (system-wide connectedness). It is also central to understanding underlying fundamental macroeconomic risks, in particular business cycle risk (e.g., intra- and inter-country real activity connectedness).

Recent theoretical work has therefore emphasized network connectedness in financial and industry contexts, as in Jackson (2008), Easley and Kleinberg (2010), Acemoglu et al. (2012), and Babus (2016). Related empirical work, which sometimes includes banking contexts, has begun to appear; see, for example, Diebold and Yilmaz (2009), Acharya, Pedersen, Philippon, and Richardson (2017), Billio, Getmansky, Lo, and Pelizzon (2012), Allen, Bali, and Tang (2012), Acharya, Engle, and Richardson (2012), Barigozzi and Brownlees (2013), Diebold and Yilmaz (2014), Brownlees and Engle (2015), Bianchi, Billio, Casarin, and Guidolin (2015), Giglio, Kelly, and Pruitt (2016), and Adrian and Brunnermeier (2016).

There is, however, little empirical research on *global* bank connectedness. This is particularly unfortunate given the role of financial institutions in the Great Recession of 2007–2009, and given the many channels that potentially produce linkages among banks, such as counter-party relationships associated with asset/liability positions, contractual relationships associated with services provided to clients and other institutions, and correlated exposures, as well as linkages via asset price and liquidity channels.[1]

A key reason for the lack of empirical work on global bank connectedness is the high dimensionality of bank networks. There are simply very many important banks globally, which renders unrestricted vector autoregressive (VAR) and related analyses intractable. Hence, for example, Diebold and Yilmaz (2014) were forced to limit their analysis to a small number of purely US institutions. Although a useful first step, such an analysis is clearly incomplete, given the global nature of the financial services industry.

[1]See, among others, the classic work of Shleifer and Vishny (1998), Allen and Gale (1994, 2000), Cifuentes, Ferrucci, and Shin (2005), Acharya and Yorulmazer (2007), and Gorton (2015).

 Copyright © 2017 John Wiley & Sons, Ltd.

In this paper we progress on both the methodological and substantive fronts. On the methodological side, we confront the dimensionality problem while nevertheless remaining squarely in the Diebold–Yilmaz connectedness measurement tradition, focusing on the degree distribution and the mean degree. We do so by estimating the network using LASSO methods, which facilitates high dimensionality by selecting and shrinking in optimal ways. We also maintain our intentionally reduced-form approach: Our goal is to provide a credible framework for "getting the facts straight," regardless of the underlying structural mechanism(s), particularly given the many mechanisms that may be operative, per the discussion above.

On the substantive side, no longer constrained by the dimensionality problem, we perform a truly global bank connectedness analysis. In particular, we characterize the static and dynamic high-frequency stock return volatility connectedness of all publicly traded banks among the world's top 150, 2004–2014.

We proceed as follows. In Section 2, we briefly summarize the Diebold–Yilmaz connectedness measurement framework. In Section 3, we introduce "LASSOed" large VARs as empirical approximating models in the Diebold–Yilmaz framework. In Sections 4 and 5, respectively, we provide static and dynamic characterizations of the global bank network, and we conclude in Section 6.

2 | POPULATION NETWORK CONNECTEDNESS

Here we discuss our connectedness framework and measures, in population. (We discuss estimation later, in Section 3.) The discussion is brief, as we use connectedness measures based on variance decompositions, as proposed and developed in a series of earlier papers that includes Diebold and Yilmaz (2009, 2012, 2014).

2.1 | Variance decompositions for connectedness measurement

Connectedness measures based on variance decompositions are appealing for several reasons. First, they make obvious intuitive sense, answering a key question, which at the most granular pairwise level is "How much of entity *i*'s future uncertainty (at horizon *H*) is due to shocks arising *not* with entity *i*, but rather with entity *j*?"

Second, they allow for different connectedness at different horizons, facilitating examination of a variety of horizons and selection of a preferred horizon if desired. This is important because, for example, 1-day connectedness may be very different from 10- or 30-day connectedness.

Finally, they are closely linked to modern network theory, in particular the degree distribution and mean degree, and they are also closely linked to recently proposed measures of various types of systemic risk, such as marginal expected shortfall (Acharya et al. 2017) and CoVaR (Adrian & Brunnermeier, 2016).[2]

2.2 | Vector autoregressive approximating models

We base our variance decomposition on an N-variable VAR(p), $x_t = \sum_{i=1}^{p} \Phi_i x_{t-i} + \varepsilon_t$, where $\varepsilon_t \sim (0, \Sigma)$. The moving average representation is $x_t = \sum_{i=0}^{\infty} A_i \varepsilon_{t-i}$, where the $N \times N$ coefficient matrices A_i obey the recursion $A_i = \Phi_1 A_{i-1} + \Phi_2 A_{i-2} + \cdots + \Phi_p A_{i-p}$, with A_0 an $N \times N$ identity matrix and $A_i = 0$ for $i < 0$.

Identification becomes challenging in the high-dimensional situations that will concern us. Standard approaches such as Cholesky factorization depend on the ordering of the variables, which raises significant complications. Hence we follow Diebold and Yilmaz (2012) in using the "generalized identification" framework of Koop, Pesaran, and Potter (1996) and Pesaran and Shin (1980), which produces variance decompositions invariant to ordering. Instead of attempting to orthogonalize shocks, the generalized approach allows for correlated shocks but accounts appropriately for the correlation.

2.3 | Connectedness measures

We now introduce our connectedness measures. We start with highly granular pairwise directional connectedness, and proceed with total directional connectedness to reach highly aggregative system-wide connectedness.

Firm *j*'s contribution to firm *i*'s *H*-step-ahead generalized forecast error variance, $\theta_{ij}^{g}(H)$, is

$$\theta_{ij}^{g}(H) = \frac{\sigma_{jj}^{-1} \sum_{h=0}^{H-1} \left(e_i' A_h \Sigma e_j\right)^2}{\sum_{h=0}^{H-1} \left(e_i' A_h \Sigma A_h' e_i\right)}, \quad H = 1, 2, \ldots, \tag{1}$$

[2]See Diebold and Yilmaz (2014) for a detailed discussion.

where Σ is the covariance matrix of the disturbance vector ε, σ_{jj} is the standard deviation of the disturbance of the jth equation, and e_i is the selection vector with one as the ith element and zeros otherwise.

Because we work in the Koop–Pesaran–Potter–Shin generalized VAR framework, the variance shares do not necessarily add to 1; that is, in general $\sum_{j=1}^{N} \theta_{ij}^{g}(H) \neq 1$. Hence we normalize each entry of the generalized variance decomposition matrix (Equation 1) by the row sum to obtain pairwise directional connectedness from firm j to firm i:

$$\tilde{\theta}_{ij}^{g}(H) = \frac{\theta_{ij}^{g}(H)}{\sum_{j=1}^{N} \theta_{ij}^{g}(H)}. \tag{2}$$

Now by construction $\sum_{j=1}^{N} \tilde{\theta}_{ij}^{g}(H) = 1$ and $\sum_{i,j=1}^{N} \tilde{\theta}_{ij}^{g}(H) = N$.

As a matter of notation, we now convert from $\tilde{\theta}_{ij}^{g}(H)$ to $C_{i\leftarrow j}^{H}$ (C is, of course, for connectedness), which is less cumbersome and more directly informative.

After obtaining the pairwise directional connectedness measure, $C_{i\leftarrow j}^{H}$, we can move to total directional connectedness measures. Total directional connectedness to firm i from all other firms j is

$$C_{i\leftarrow \bullet}^{H} = \frac{\sum_{\substack{j=1 \\ j\neq i}}^{N} \tilde{\theta}_{ij}^{g}(H)}{\sum_{i,j=1}^{N} \tilde{\theta}_{ij}^{g}(H)} = \frac{\sum_{\substack{j=1 \\ j\neq i}}^{N} \tilde{\theta}_{ij}^{g}(H)}{N}. \tag{3}$$

Similarly, total directional connectedness from firm i to all other firms j is

$$C_{\bullet\leftarrow i}^{H} = \frac{\sum_{\substack{j=1 \\ j\neq i}}^{N} \tilde{\theta}_{ji}^{g}(H)}{\sum_{i,j=1}^{N} \tilde{\theta}_{ji}^{g}(H)} = \frac{\sum_{\substack{j=1 \\ j\neq i}}^{N} \tilde{\theta}_{ji}^{g}(H)}{N}. \tag{4}$$

Finally, we obtain the system-wide connectedness measure. Using the normalized entries of the generalized variance decomposition matrix (Equation 2), we measure total directional connectedness as

$$C^{H} = \frac{\sum_{\substack{i,j=1 \\ i\neq j}}^{N} \tilde{\theta}_{ij}^{g}(H)}{\sum_{i,j=1}^{N} \tilde{\theta}_{ij}^{g}(H)} = \frac{\sum_{\substack{i,j=1 \\ i\neq j}}^{N} \tilde{\theta}_{ij}^{g}(H)}{N}. \tag{5}$$

We call this total connectedness *system-wide* connectedness. It is simply the sum of total directional connectedness whether "to" or "from." (It doesn't matter which way, because "exports" must equal "imports" at the "global" level.)

3 | SAMPLE BANK NETWORK CONNECTEDNESS

Thus far we have discussed population network connectedness measurement. Now we discuss *sample* connectedness measurement, specialized, moreover, to the context of global banking, which we study in detail in Sections 4 and 5.

3.1 | Banks, sample period, and stock return volatilities

We study 96 banks from 29 developed and emerging economies, downloaded from Thomson-Reuters, from September 12, 2003 to February 7, 2014. Our 96 banks are those in the world's top 150 (by assets) that were publicly traded throughout our sample. They are largely banks from developed countries: 82 are from 23 developed economies, and the remaining 14 are from six emerging economies.[3] They include all those designated as "globally systemically important banks" ("GSIBs," as designated by the Basel Committee on Banking Supervision), except for three Chinese banks (Agricultural Bank of China, Bank of China, and Industrial and Commercial Bank of China) and one French bank (Group BCPE), which we exclude because they were not publicly traded as of September 2003.

[3]See the online appendices for details regarding market capitalization, bank code, and Reuters ticker, by bank assets (Supporting Information Appendix A) and by country (Supporting Information Appendix B). Our bank codes are easier to interpret than the Reuters tickers, particularly as regards identifying banks' countries, so we use them in our subsequent empirical work.

We focus on connectedness in the global bank stock return volatility network, which does not require high-frequency balance sheet and related information, which is unavailable in real time. Instead we need only high-frequency stock return data, which are readily available. Stock market valuations are, of course, imperfect—like all valuations—but equity analysts devote massive time and resources to uncovering and interpreting connectedness information as relevant for valuation.

Volatility connectedness is of direct interest in financial markets. If volatility tracks investor fear (e.g., the VIX is often touted as an "investor fear gauge"), then volatility connectedness is fear connectedness. Hence volatility connectedness is of special interest from the perspective of real-time crisis monitoring, as volatilities tend to lurch and move together only in crises, whereas returns often move closely together in both crises *and* upswings.

Volatility is latent and must therefore be estimated. Many approaches to volatility estimation have received attention, including generalized autoregressive conditional heteroskedasticity, stochastic volatility, realized volatility, and implied volatility.[4] We use daily range-based realized volatility. That is, following Garman and Klass (1980), we estimate daily bank stock return volatility as

$$\begin{aligned}\tilde{\sigma}_{it}^2 = {} & 0.511(H_{it} - L_{it})^2 - 0.019[(C_{it} - O_{it})(H_{it} + L_{it} - 2O_{it}) \\ & - 2(H_{it} - O_{it})(L_{it} - O_{it})] - 0.383(C_{it} - O_{it})^2,\end{aligned} \tag{6}$$

where H_{it}, L_{it}, O_{it}, and C_{it} are, respectively, the logs of daily high, low, opening, and closing prices for bank stock i on day t. Range-based realized volatility is nearly as efficient as realized volatility based on high-frequency intra-day sampling, yet it requires only four readily available inputs per day, and it is robust to certain forms of microstructure noise (Alizadeh, Brandt, and Diebold, 2002).

Finally, we note that our bank stock price data come from markets located in different time zones. Although this could potentially influence the empirical results, the use of return volatilities rather than returns, and the use of a VAR approximating model, are likely to minimize the potential impact. In particular, our use of volatility in the connectedness analysis helps to identify the origins of shocks, as volatility jumps more during crises, as does our use of a vector autoregressive approximating model, to which we now turn.

3.2 | Estimation of high-dimensionsal VARs

In applications we base connectedness assessment on an estimated VAR approximating model. For compelling applications, we need the VAR to be estimable in high dimensions, somehow recovering degrees of freedom.[5] One can do so by pure shrinkage (as with traditional informative-prior Bayesian analyses, or ridge regression) or pure selection (as with traditional criteria like Akaike information criterion and Schwartz information criterion), but *blending* shrinkage and selection, using variants of the LASSO, proves particularly appealing.

To understand the LASSO, consider least-squares estimation:[6]

$$\hat{\beta} = \arg\min_{\beta} \sum_{t=1}^{T} \left(y_t - \sum_i \beta_i x_{it} \right)^2, \tag{7}$$

subject to the constraint:

$$\sum_{i=1}^{K} |\beta_i|^q \leqslant c.$$

Equivalently, consider the penalized estimation problem:

$$\hat{\beta} = \arg\min_{\beta} \left[\sum_{t=1}^{T} \left(y_t - \sum_i \beta_i x_{it} \right)^2 + \lambda \sum_{i=1}^{K} |\beta_i|^q \right]. \tag{8}$$

Concave penalty functions non-differentiable at the origin produce selection, whereas smooth convex penalties (e.g., $q = 2$, the ridge regression estimator) produce shrinkage. Hence penalized estimation nests and can blend selection and shrinkage.

[4]For a survey see Andersen, Bollerslev, Christoffersen, and Diebold (2013).
[5]In what follows we refer to estimators that achieve this as "regularized," and associated environments as involving "regularization."
[6]We present LASSO for a generic regression equation $y \to X$, to maximize notational transparency. In our subsequent equation-by-equation VAR estimation, the right-hand-side variables in each equation are, of course, p-lags of each of the N variables.

FIGURE 1 Network graph color spectrum [Colour figure can be viewed at wileyonlinelibrary.com]

The LASSO (short for "least absolute shrinkage and selection operator"), introduced in the seminal work of Tibshirani (1996), solves the penalized regression problem with $q = 1$. Hence it shrinks and selects. Moreover, it requires only one minimization, and it uses the smallest q for which the minimization problem is convex.

A simple extension of the LASSO, the so-called adaptive elastic net (Zou & Zhang, 2009), not only shrinks and selects, but also has the oracle property, meaning (roughly) that the selected model is consistent for the best Kullback–Liebler approximation to the true DGP. In our implementation of the adaptive elastic net, we solve

$$\hat{\beta}_{\text{AEnet}} = \arg\min_{\beta} \left[\sum_{t=1}^{T} \left(y_t - \sum_{i} \beta_i x_{it} \right)^2 + \lambda \sum_{i=1}^{K} w_i \left(\frac{1}{2}|\beta_i| + \frac{1}{2}\beta_i^2 \right) \right], \tag{9}$$

where $w_i = 1/|\hat{\beta}_{i,\text{OLS}}|$ and λ is selected equation by equation by 10-fold cross-validation. Note that the adaptive elastic net penalty averages the "LASSO penalty" with a "ridge penalty," and, moreover, that it weights the average by inverse ordinary least squares (OLS) parameter estimates, thereby shrinking the "smallest" OLS-estimated coefficients most heavily toward zero.[7]

Before ending this section, we would like to address two issues related to our empirical estimation approach. First, we want to encourage sparsity in our approximating model, but we do not necessarily want to impose sparsity in the implied bank network. Our approach of shrinking and selecting on the approximating VAR, as opposed to shrinking and selecting on the variance decomposition network directly, achieves that goal. The approximating VAR is intentionally shrunken and made sparse by the LASSO, but the variance decomposition matrix that drives our connectedness measures is a nonlinear transformation of the VAR coefficients and is therefore generally not sparse.[8]

Second, we regularize the estimated VAR coefficient matrices, but currently we do not pursue regularization of the shock covariance matrix, in large part because we are not necessarily comfortable with the standard "statistical" shrinkage directions (e.g., toward zero). Instead, one might want to shrink and select in other directions, such as toward equicorrelation or reduced-rank structure, but we leave covariance matrix regularization to future research.

3.3 | Network visualization of high-dimensional variance decompositions

The issue of how best to display results takes on great importance in high-dimensional network modeling. In our subsequent empirical work, for example, we will estimate networks with approximately 100 nodes, and presenting and examining $100 \times 100 = 10,000$ estimated pairwise variance decompositions would be thoroughly uninformative. Hence we characterize the estimated networks graphically using five devices: node naming convention, node size, node color, node location, and link arrow sizes (two per link, because the network is directed). Throughout, we use the open-source Gephi software (https://gephi.github.io/) for network visualization.

Node naming convention indicates bank and country The node naming convention is bank.country, where "bank" is our bank code and "country" is our country code. For example, J. P. Morgan is jpm.us.[9]

Node size indicates asset size We make node size a linear function of bank asset size.[10] We assign the sizes of the largest and smallest nodes, and then assign the rest linearly. We emphasize assets rather than market capitalization for two reasons. First, market capitalization is subject to abrupt changes due to fluctuations in stock price. Second, cross-country differences in financial system characteristics and ownership structure of publicly traded companies have direct effects on market capitalization levels, thereby producing persistent differences in cross-country market capitalizations.

Node color indicates total directional connectedness "to others" The node color indicates total directional connectedness to others, ranging from 3DFA02 (bright green, the weakest), to E6DF22 (luminous vivid yellow), to CF9C5B (whiskey sour), to FC1C0D (bright red), to B81113 (dark red, the strongest). We show the color range in Figure 1.

[7]The weighting by inverse estimates is responsible for the oracle property.
[8]Alternative frameworks that attempt to characterize network connectedness directly from a fitted sparse VAR(1) coefficient matrix (e.g., Bonaldi, Hortacsu, and Kastl, 2015) force sparse networks, by construction. Moreover, they also provide incomplete connectedness characterizations, because VAR connectedness arises not only through cross-lag linkages but also through the disturbance covariance matrix. Network connectedness measures based on Granger-causal patterns (e.g., Billio et al., 2012) also ignore the disturbance covariance matrix and hence are similarly incomplete.
[9]The other bank and country codes are similarly self-evident; see the online appendices for a complete listing.
[10]Note well that we make node size and asset size linearly related, but not directly proportional. Huge asset size differences between the largest and smallest banks in our sample make directly proportional representation impossible.

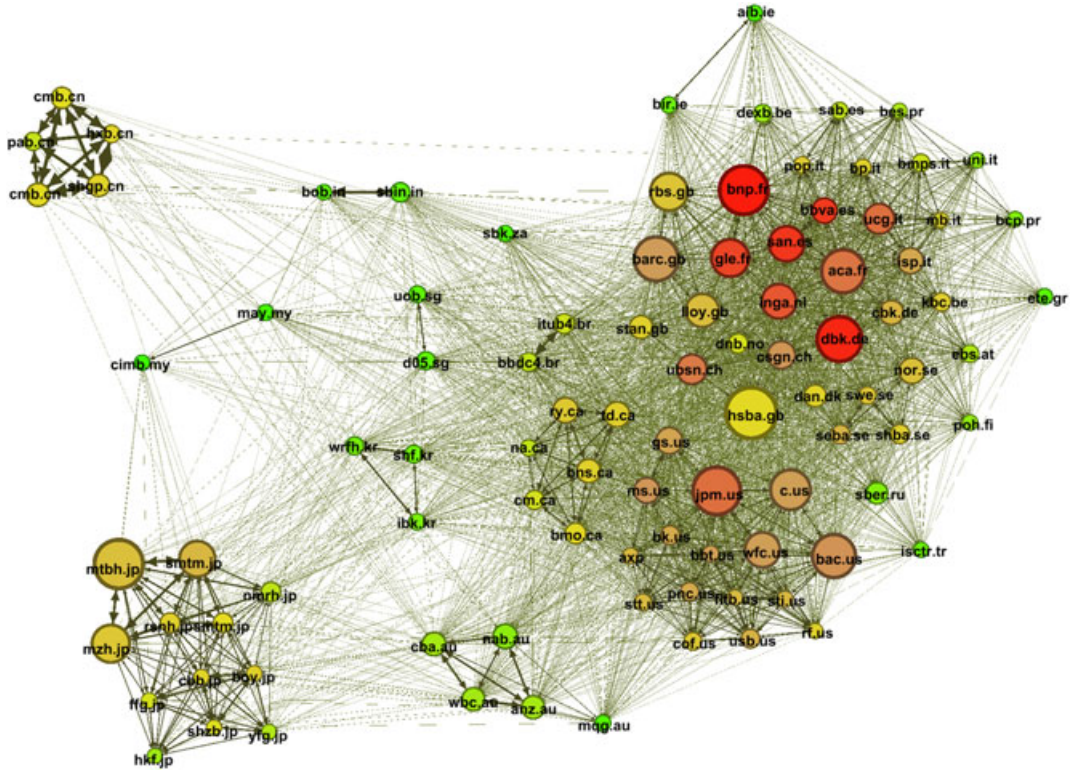

FIGURE 2 Individual bank network graph, 2003–2014 [Colour figure can be viewed at wileyonlinelibrary.com]

Node location indicates average pairwise directional connectedness[11] We determine node location using the ForceAtlas2 algorithm of Jacomy, Heymann, Venturini, Bastian (2014) as implemented in Gephi. The algorithm finds a steady state in which repelling and attracting forces exactly balance, where nodes repel each other like similar poles of two magnets, while links, like springs, attract their nodes. Here the attracting force of a link is proportional to average pairwise directional connectedness "to" and "from." The steady-state node locations depend on initial node locations and hence are not unique. This is largely irrelevant, however, as we are interested in relative, not absolute, node locations in equilibrium.

Link arrow sizes indicate pairwise directional connectedness "to" and "from" Note that because the full set of link arrow sizes reveals the full set of pairwise directional connectednesses, from which all else can be derived, most of the additional graphical devices employed (in particular, node shading and location) are in principle redundant and therefore unnecessary. In practice, however, those additional devices prove invaluable for describing large network topologies.

4 | STATIC ESTIMATION OF THE GLOBAL BANK NETWORK

We estimate logarithmic volatility VARs using the adaptive elastic net as described above. Then we compute variance decompositions and corresponding connectedness measures at horizon $H = 10$, using the estimated VAR parameters.

4.1 | The individual bank network

We show the full-sample global bank network graph in Figure 2. The main result is the strong clustering, both within and across countries.[12] The within-country bank clustering is ubiquitous, ranging from countries with many banks in our sample (e.g., USA, Canada, Australia, China, Japan) to those with only two or three (e.g., Korea, Singapore, India, Malaysia). The cross-country clustering is also obvious throughout the graph, whose left side clearly tends to contain banks of eastern countries,

[11] Link thickness also indicates average pairwise directional connectedness.

[12] A second interesting result is the high coherence between banks designated as GSIBs and those that we estimate and display as having high net total directional connectedness ("to" minus "from," $C^H_{\bullet \leftarrow i} - C^H_{i \leftarrow \bullet}$). When we sort banks by net connectedness, all of our top 15 banks are included in the GSIB list, as are 20 of our top 25.

TABLE 1 Individual bank network connectedness table, six-group aggregation, 2003–2014

	Africa	Asia	Europe	N. America	Oceania	S. America	From others
Africa	0.00	8.51	18.78	13.84	1.77	2.14	45.05
Asia	4.08	0.00	205.03	157.42	30.22	21.90	418.64
Europe	6.62	93.44	0.00	431.31	20.57	29.31	581.25
N. America	3.14	58.72	417.83	0.00	20.63	26.91	527.24
Oceania	2.00	39.67	68.08	74.44	0.00	5.27	189.46
S. America	1.38	14.29	48.41	48.34	2.63	0.00	115.06
To others	17.20	214.65	758.13	725.35	75.84	85.53	312.78

and whose right side clearly tends to contain banks of western countries. Moreover, the western side clearly breaks into a large Anglo/European bank cluster and a smaller American/Canadian cluster, each of which contains sub-clusters.

It is not obvious that region of origin would be the dominant factor driving network connectedness. One might have thought, for example, that other factors, such as bank size, might dominate, but such is not the case. Japan illustrates this clearly. Although the majority of very large banks are located in the Anglo/American/European cluster, the three very large Japanese banks (Mitsubishi UFJ, Mizuho Financial, and Sumitomo Mitsui Financial) are located not in the Anglo/American/European cluster, but rather in the Japanese cluster.

Given the clear regional clustering in the network graph, we show in Table 1 a six-region network connectedness table. The main elements are the pairwise directional connectednesses defined in Equation 2, the row sums labeled "from others" are the total directional connectednesses from others defined in Equation 3, the column sums labeled "to others" are the total directional connectednesses to others defined in Equation 4, and the lower right element is the system-wide connectedness defined in Equation 5. The table's message is clear: North America and Europe are large (and indeed the only) net transmitters of future volatility uncertainty ("to others"—"from others") to the rest of the world. Asia also has noticeably large total directional connectedness—both large transmissions and large receipts (i.e., total directional connectedness "to" and "from")—but at this point it remains a clear net receiver.

4.1.1 | Including sovereign bonds

Thus far we have analyzed the global network of bank equity return volatilities, but we can also include other important financial asset volatilities. This is potentially interesting because, although the US financial crisis did not have a sovereign debt component, the ensuing European crisis did.

Against this background, we now briefly include sovereign bond yield volatilities in the analysis, in addition to bank stock volatilities. We include 10-year G-7 sovereigns (USA, Germany, France, Japan, UK, Canada, and Italy), as well as those of Spain, Greece, and Australia. We start with government bond prices, and then we convert to approximate yields using $P_t = 1/(1+r_t)^{10}$, where P_t is price and r_t is 10-year yield. Then we calculate daily range-based return volatilities using the Parkinson (1980) approach, which requires only the daily highs and lows (as opposed to high, low, open, and close). That is, we use $\tilde{\sigma}_{it}^2 = 0.361(H_{it} - L_{it})^2$, where H_{it} and L_{it} are, respectively, the logs of daily high and low prices for bank stock i on day t.

We plot the estimated individual bank/sovereign bond network in Figure 3. Several observations are in order. First, the sovereigns cluster strongly. They appear in the upper right of the graph, which is otherwise similar to Figure 2.[13] Second, European bond nodes are nevertheless closer to European bank nodes, US and Canadian bond nodes are closer to US and Canadian bank nodes, and Japanese and Australian bond nodes are closer to Japanese and Australian bank nodes. Third, although the bond nodes are pulled toward their respective country bank nodes, they remain completely distinct and never appear inside their national/regional banking clusters: bank stocks form regional/national clusters, and sovereign bonds are not part of those clusters.

4.2 | The country bank network

In Figures 4 and 5 (without and with sovereign bonds included, respectively) we show the country bank network obtained by aggregating the earlier-discussed individual bank network.[14] This serves two useful and distinct purposes.

[13]The country bond node naming convention is `COUNTRY_b`, where "COUNTRY" is our country code (capitalized) and "b" denotes bond. For example, the US government bond is `USA_b`. The other country codes are generally similarly self-evident; see the online appendices for a complete listing.
[14]We place country nodes at the centers of gravity of the corresponding country banks.

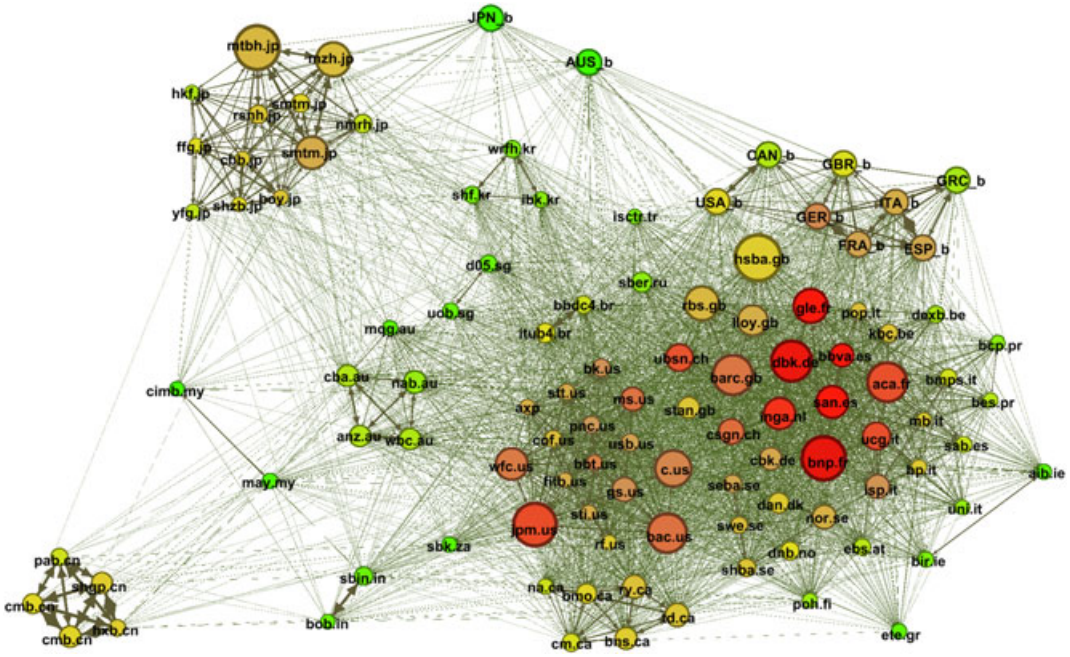

FIGURE 3 Individual bank/sovereign bond network, 2003–2014 [Colour figure can be viewed at wileyonlinelibrary.com]

FIGURE 4 Country bank network, 2003–2014 [Colour figure can be viewed at wileyonlinelibrary.com]

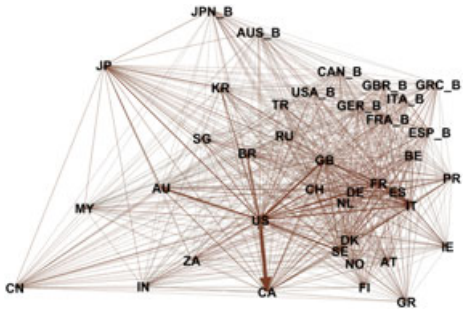

FIGURE 5 Country bank/sovereign bond network, 2003–2014 [Colour figure can be viewed at wileyonlinelibrary.com]

First, examination of the country bank network is intrinsically interesting and a logical next step. Our individual-bank analysis showed strong connectedness of banks both within and across countries, so we now proceed to dig more deeply into the cross-country links. Examination of the country bank network allows us to distinguish the relative strengths of directional "to" and "from" connectedness of the most-connected country banking systems.

Second, the smaller number of links in the country bank network makes visual interpretation of connectedness simpler and more revealing. (29 countries produce only $29^2 = 841$ links in the country network, whereas 96 banks produce $96^2 = 9,216$ links in the bank network.)

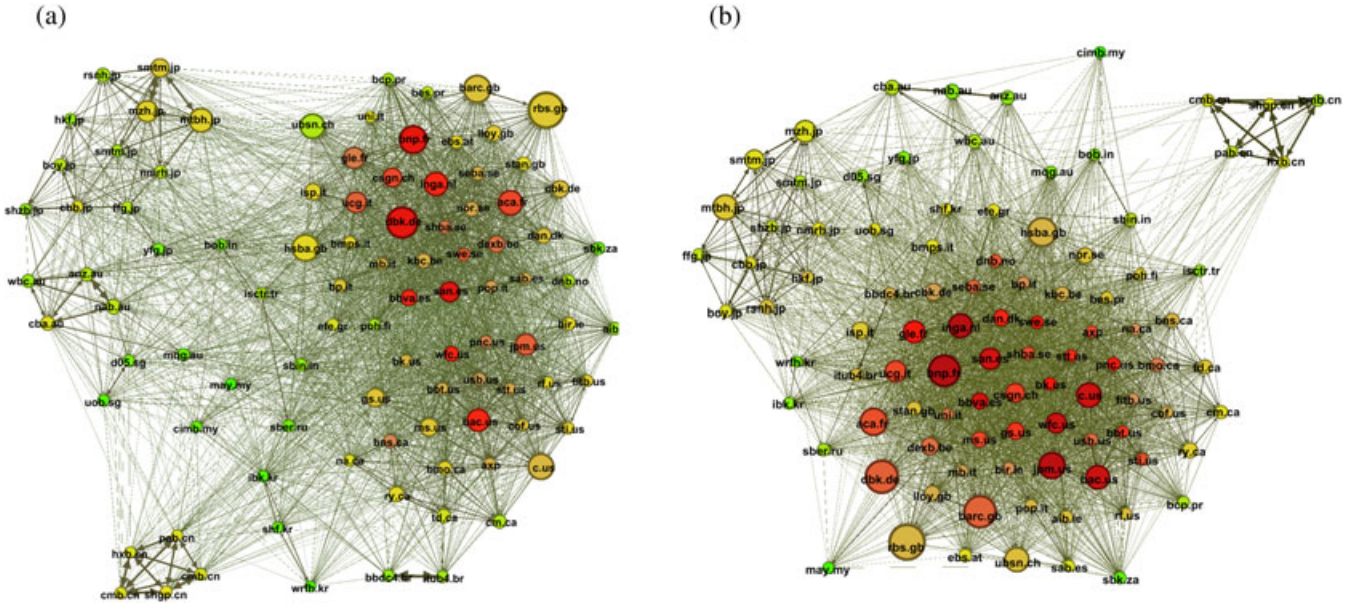

FIGURE 6 Individual bank network pre- and post-Lehman: (a) September 1, 2008; (b) November 21, 2008 [Colour figure can be viewed at wileyonlinelibrary.com]

The equity volatility network of Figure 4 reveals that the USA is massively connected. The strongest US links are with Canada, Great Britain, and Australia. It is not always visible, but the arrows indicate greater connectedness from the USA to Canada, Australia, and Great Britain than conversely. The Anglo/European countries form a cluster just above the USA. Of the Anglo/European countries, Britain has the strongest links to and from the USA. The northern European countries are to the southeast of the cluster; Sweden has the strongest connectedness with the USA. Ireland, Portugal, Greece, Finland, and Austria are located on the perimeter of the cluster. Other countries are scattered farther away from the European cluster. As noted previously for individual banks, moving leftward on the graph generally takes one from western to eastern countries. Finally, the equity/bond volatility network of Figure 5 reveals that, as in the individual bank analysis, the bonds cluster tightly, regardless of geography.

5 | DYNAMIC ESTIMATION OF THE GLOBAL BANK NETWORK

We now characterize the global banking network dynamically. We use rolling estimation with a 150-day window, with repeated cross-validation of the penalty parameter λ in each window.[15] We start with comparisons of estimated network graphs "before and after" major crisis episodes, and then we proceed to examine the continuous real-time evolution of system-wide connectedness.

5.1 | Banks pre- and post-Lehman

The critical point in the financial crisis was Lehman's bankruptcy, which was announced on September 15, 2008. In Figure 6 we show the 96-bank network graphs on September 1, 2008 and on November 21, 2008. There is a clear difference between the individual bank network graphs on the two dates.

In particular, connectedness of US banks with others increased sharply after Lehman's collapse and the transformation of the US financial crisis into a global one. Before the Lehman collapse, the US and European banks stood far apart around the Anglo/American/European cluster, with a visible gap in the network graph between the US and European banks. The Japanese and Chinese banks also stood apart. Once the Lehman shock hit global markets, the entire individual bank network, perhaps with the exception of Chinese banks, moved closer together, indicating the spread of volatility across bank stocks and countries.

[15]For rolling estimation we switch from adaptive elastic net to elastic net, meaning that we use $w_i = 1$ rather than $w_i = 1/|\hat{\beta}_{i,\mathrm{OLS}}|$ in the estimator (Equation 9), because we found that the elastic net produces less noisy estimates under rolling estimation.

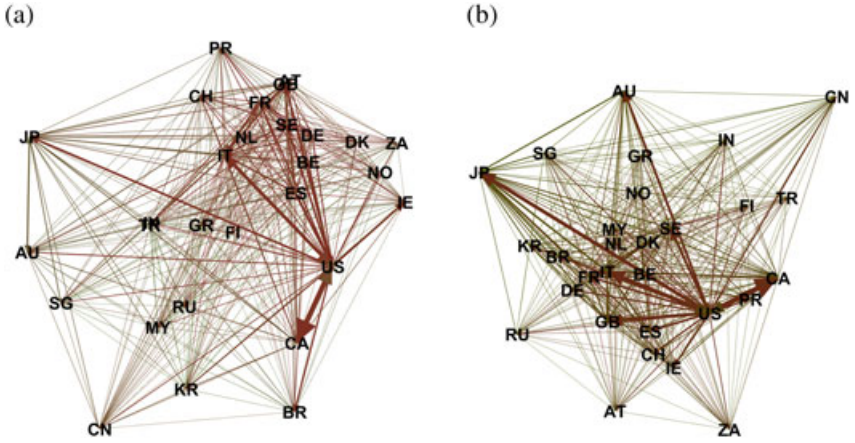

FIGURE 7 Country bank network pre- and post-Lehman: (a) September 1, 2008; (b) November 21, 2008 [Colour figure can be viewed at wileyonlinelibrary.com]

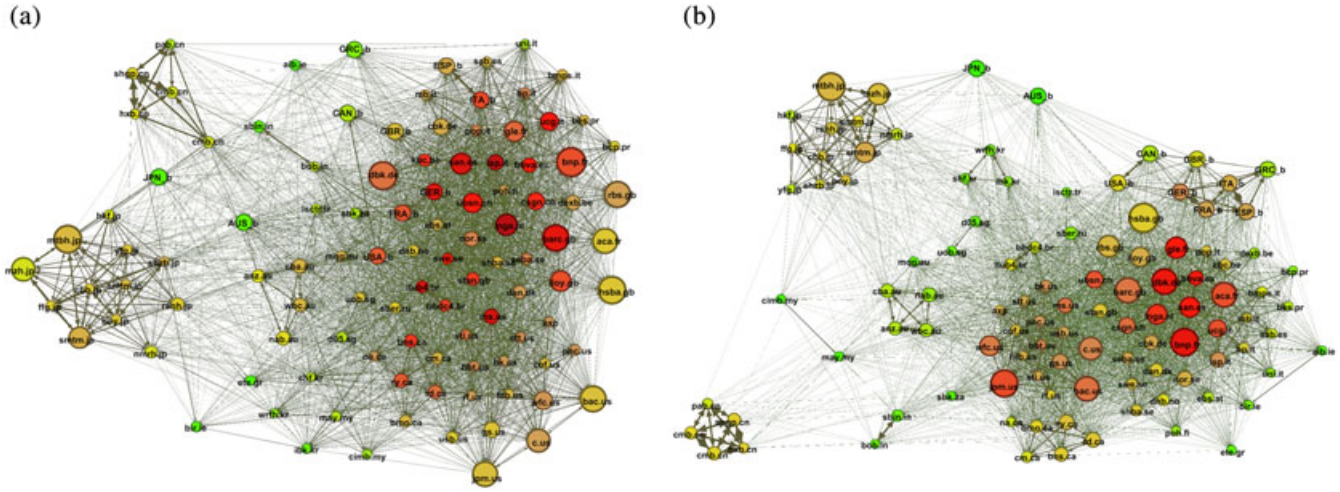

FIGURE 8 Individual bank/sovereign bond network, full-sample versus after the European crisis: (a) rolling estimation, 150-day window ending October 7, 2011; (b) full-sample estimation [Colour figure can be viewed at wileyonlinelibrary.com]

It is important to stress that volatility data coming from stock markets operating in different time zones does not prevent our framework from capturing the sharp increase in pairwise directional connectedness after the collapse of Lehman Brothers.

A similar picture arises when we analyze the country bank network before and after Lehman's collapse. We show the country bank network graphs in Figure 7. Connectedness was comparatively weak before the collapse, and much stronger afterward. Moreover, the directional volatility connectedness from the USA to others increased substantially.

5.2 | Banks, bonds, and the European debt crisis

To see how the individual bank/sovereign bond network was transformed following the European banking and sovereign bond crisis, we analyze the network graph once the European sovereign debt and banking crisis spread throughout the continent, affecting mostly the periphery countries such as Greece, Portugal, Ireland, Italy and Spain. However, sovereign bonds of the center countries such as Germany, France, and Great Britain could not be isolated from the events unfolding in the periphery. As a result, on October 7, 2011 connectedness reached its highest level since the global financial crisis of late 2008.[16]

In Figure 8(a) we show the October 2011 individual bank/sovereign bond network, and in Figure 8(b) we once again show the full-sample network for comparison. The graphs are quite different. The October 2011 bond yield volatilities are no longer on the outskirts of the regional/national banking clusters. Indeed, bond yield volatilities for the USA, UK, Germany, and France moved toward the center of the European/North American banking cluster. Italy and Spain did not move to the center of the

[16]More precisely, system-wide connectedness peaked on October 7, 2011, as shown in Figure 9.

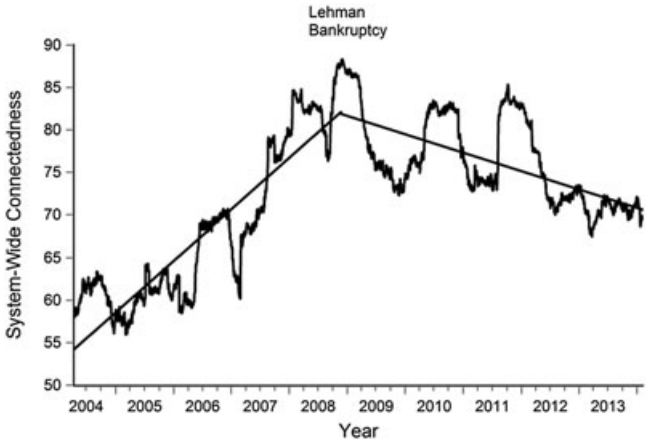

FIGURE 9 System-wide connectedness, with superimposed trend

cluster, but they are still closer to the center of the Anglo/American/European cluster than they were in the full sample. Greek bonds, on the other hand, are separated from other sovereign bonds (including the European bonds) as well as individual banks.[17] Australian bonds moved closer to the Japanese bonds. Furthermore, the nodes for the Japanese and Chinese banks, as well as those from other countries, moved closer to the Anglo/American/European cluster, indicating stronger volatility connectedness in October 2011 compared to the full sample.

All told, Figure 8 clearly shows that the European banking and sovereign debt crises had become intertwined as of October 2011. The US banks are farther away from the center of the Anglo/American/European cluster, and the European banks are at the center, close to the government bond markets of the USA, France, Germany, and the UK.

5.3 | System-wide connectedness

Now we consider system-wide connectedness. There are two interesting ways to display and decompose it: trend versus cycle and cross-country versus within-country. We consider them in turn.

5.3.1 | Trend and cycle

We first display and decompose dynamic system-wide connectedness into secular (trend) and cyclical variation, as shown in Figure 9. As indicated by the superimposed piecewise linear trend, system-wide connectedness broadly increased for roughly the first half of our sample, peaking with the Lehman bankruptcy. It then decreased gradually, albeit with some major bumps associated with the two waves of the European debt crisis, falling by almost 20 percentage points relative to its peak by the end of the sample.

Let us first discuss aspects of the pre-Lehman episode. First, the connectedness of major global bank stocks increased following the Fed's unexpected decision to tighten monetary policy in May and June 2006. However, there was no other major volatility shock across the global banking system in 2006, so that estimated connectedness subsides as the observations for May–June 2006 vanish from the rolling window. Volatility connectedness was low in early 2007. However, following the collapse of several mortgage originators in the USA, connectedness increased sharply. This jump was followed by an even greater jump during the liquidity crisis of August 2007, when it became apparent that along with the US banks the European banks also had to write off billions of dollars of losses due to their investments in mortgage-backed securities. By the end of 2007, it became apparent that the major US banks would end up writing off tens of billions of dollars in losses. Then in March 2008, Bear Stearns, one of the top US investment banks, was acquired by J. P. Morgan to avoid bankruptcy.

Now consider the post-Lehman episode. System-wide connectedness reached its peak following the Lehman bankruptcy on September 15, 2008, at which time the US government introduced a huge package of direct capital injection into major US banks. As months passed, the US markets calmed, and system-wide connectedness started to trend downward. However, in 2009 and 2010 the EU member countries were shocked by developments in the banking and sovereign debt markets of some of its

[17] We believe that this is a reflection of the declining exposure of the European banks to Greek sovereign bonds from EUR 189 billion at the beginning of 2010 to EUR 104 billion at the end of 2011. (Sources: BIS *Quarterly Review*, June 2010 and June 2012, Table 9B).

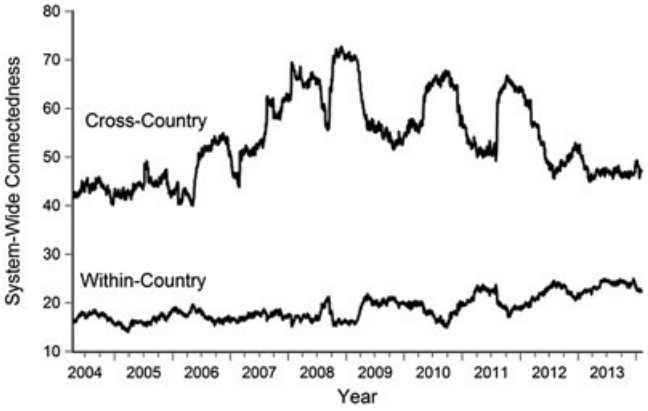

FIGURE 10 System-wide connectedness, cross-country and within-country

peripheral member countries, including Greece, Ireland, and Portugal. Then in 2011, Italy and Spain joined the countries with stressed banking systems and sovereign bond markets. As a result, system-wide connectedness experienced two more significant jumps in May 2010 (due to delay in the rescue package for Greece) and in July–August 2011 (due to spread of sovereign debt and banking sector worries to Spain and Italy).

In closing this section, it may be useful to offer conjectures regarding not only aspects of the connectedness increase during the 2007–2008 crisis, but also regarding the subsequent connectedness decrease, and similarly for the various European debt crises. Connectedness could have increased more in the weeks after the Lehman collapse had the US government decided not to rescue AIG. Moreover, connectedness decreased more quickly in the months after Lehman's collapse as the US government used the USD 700 billion Troubled Asset Relief Program (TARP) to inject capital into the major US banks. That decision helped increase confidence in the US banking system and hence prevented a potential breakdown of the global financial system. Finally, stress test results also indicated that US banks were sound and led to a significant decline in system-wide connectedness in 2009. As for subsequent crises, in the Greek debt crisis of 2009–2010 the ECB/IMF/EC rescue package proved effective, and in the European banking and sovereign debt crisis of 2011 the intervention of ECB under the new president Mario Draghi eventually brought down system-wide connectedness, as the ECB announced a 3-year EUR 1 trillion Long-term Refinancing Operation (LTRO) package that provided liquidity to many of the banks that had difficulty in borrowing in the overnight market.

5.3.2 | Cross-country and within-country

A second way to display and decompose dynamic system-wide connectedness involves cross-country and within-country parts, as in Figure 10. Cross-country system-wide connectedness is the sum of all pairwise connectedness across banks located in different countries. Within-country system-wide connectedness is the sum of pairwise connectedness across banks in the same country. By construction, cross-country and within-country system-wide connectedness must sum to system-wide connectedness. The decomposition is of interest because exploring the country origins of volatility shocks and their temporal evolution may help us better understand the dynamics of global bank connectedness.

The decomposition shows that most movements in system-wide connectedness are due to movements in cross-country system-wide connectedness. Cross-country system-wide connectedness is around 40% from 2004 to May 2006, but it then begins to fluctuate significantly. Following the Fed's unexpected decision to further tighten US monetary policy, cross-country system-wide connectedness increases by around 15% in May–December 2006. Following this episode, cross-country connectedness continues to vary throughout the sample.

It is interesting to note the decline in within-country connectedness in 2008:Q4.[18] We conjecture that there are at least two reasons. First, US intervention following the Lehman collapse likely increased confidence in the US financial system and reduced within-US connectedness in 2008:Q4. As there are 16 US banks in our analysis, the decline in within-US connectedness induces a decline in the overall within-country connectedness. The second reason follows from the simple arithmetic of connectedness. System-wide connectedness is equal to the sum of cross-country and within-country connectedness. Once the US financial crisis was transformed into a global one in the last quarter of 2008, cross-country connectedness increased sharply, with US banks spreading shocks to European banks. At that point the system-wide connectedness was already 88%, and we know that it is bounded above by 100. As it approaches 100 it takes smaller steps. Therefore, as the cross-country connectedness increases

[18]We thank a referee for pointing this out.

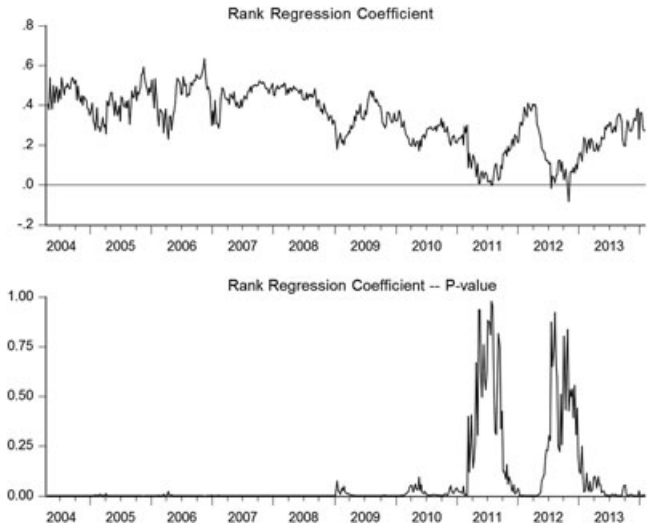

FIGURE 11 Rank regression of eigenvector centrality on market capitalization

sharply, the within-country connectedness becomes less important and hence declines. A similar dynamic appears in 2010 and 2011 during the European sovereign debt and banking crises.

5.4 | Size and eigenvector centrality

One of the primary goals of network analysis is evaluating the relative importance of individual network members. This is highly relevant for our global banking network because, as shown during the recent global financial crisis, an individual bank may be the source of financial stress that can be transmitted to the whole system. Furthermore, from a policy viewpoint, detecting such systemically important financial institutions carries enormous importance in preventing future crises.

In Diebold and Yilmaz (2014) and thus far in this paper, we emphasized total directional connectedness to others for ranking systemically important institutions.[19] But that captures only one-step links, whereas there may be multi-step links as well.[20] To explore this, we calculate the eigenvector centrality S_t, which measures the influence of a bank by incorporating connectedness of its neighbors, for each bank in our sample. S_t satisfies

$$S_t = C_t\, S_t, \tag{10}$$

where S_t is the $N \times 1$ vector of bank eigenvector centralities and C_t is the $N \times N$ network connectedness (adjacency) matrix. The solution for S_t in Equation 10 corresponds to the eigenvector associated with the largest eigenvalue of C_t. More intuitively, note that Equation 10 makes clear that the eigenvector centrality for a given bank is equal to the sum of the centralities of the connected banks weighted by the sizes of the respective links.

From our earlier-estimated time series of C_t, we can calculate the corresponding series of estimated S_t, which then allows us to investigate the dynamic interaction between bank market capitalization and centrality. Toward that objective, we estimate the cross-section rank regression of bank centrality on market capitalization for each subsample window.[21] Figure 11 presents the rank regression coefficient and its p-value over the rolling windows. In line with expectations, bank eigenvector centrality is highly correlated with bank size, with the regression coefficient fluctuating between 0.4 and 0.6 in 2004 and 2005. More importantly, however, the relationship between centrality rank and size rank weakens during the global financial crisis of 2008–2009. It even disappears completely during the second phase of the European debt crisis in summer 2011 and late 2012, when the coefficient p-value moves well above the 5% level.

On the basis of this evidence we can conclude that, whereas the largest banks are more likely to be central in the global financial system in good times, smaller banks can also become central during bad times and generate volatility connectedness that will have systemic implications.

[19]In Diebold and Yilmaz (2014) we also noted the close relationship between CoVaR (Adrian & Brunnermeier, 2016) and total directional connectedness to others.

[20]For example, banks A and C may not be directly (one-step) linked, but A may be linked to B, and B to C, so that A and C are indirectly linked (in this example, two-step linked).

[21]The series we use in our rank regression analysis is measured at weekly frequency, rather than the daily frequency used throughout the rest of the paper. For conversion we use end-of-week centralities and capitalizations.

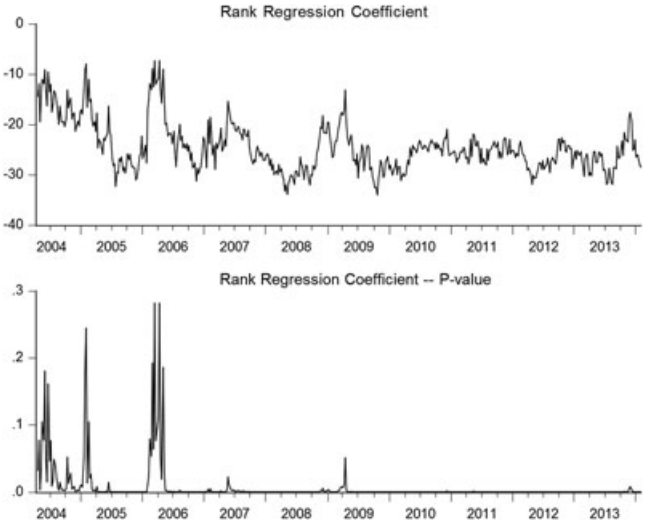

FIGURE 12 Regression of eigenvector centrality rank on GSIB dummy

So far in this section we have focused on the relationship between banks' market capitalization and eigenvector centrality in the volatility network. Alternatively, we can focus on the relationship between banks' GSIB status and eigenvector centrality. Towards that end, we regress the eigenvector centrality rank of banks on a constant term along with a dummy that indicates whether the bank is included in the GSIB list at the beginning of that year. Figure 12 reports the evolution of the estimated coefficient and its *p*-value. The negative coefficient estimate on the GSIB dummy indicates that GSIBs are likely to be more central (higher eigenvector centrality measure) than non-GSIBs. Except for a short time in the pre-crisis period (2004–2006), the central position of GSIBs in the network tends to be statistically significant. An average of −26 for the coefficient estimate from mid-2006 onward indicates that, everything else equal, a GSIB is likely to be ranked 25 banks ahead of a non-GSIB when ranked according to the eigenvector centrality measure.

6 | CONCLUSION

We have used LASSO methods to shrink, select, and estimate the high-dimensional network linking the publicly traded subset of the world's top 150 banks, 2003–2014. We characterized static network connectedness using full-sample estimation and dynamic network connectedness using rolling-window estimation. Statically, we found that global bank equity connectedness has a strong geographic component, whereas country sovereign bond connectedness does not. Dynamically, we found that equity connectedness increases during crises, with clear peaks during the Great Financial Crisis and each wave of the subsequent European Debt Crisis, and with movements coming mostly from changes in cross-country as opposed to within-country bank linkages.

ACKNOWLEDGMENTS

For constructive comments and guidance we thank Jonathan Wright, the Editor, and two referees. For helpful discussion we thank seminar participants at CORE, National Bank of Belgium, Duke University, the European University Institute, the International Monetary Fund, the PIER Policy Tools Workshop, Université Catholique de Louvain, the University of York, Koç University, the University of Pennsylvania, the University of Minho, Bogazici University, the University of Bologna, the University of Delaware, and the Federal Reserve Bank of Richmond. We are similarly grateful to participants at the University of Chicago Conference on Machine Learning and Economics, ECB-CBRT Conference on Assessing the Macroeconomic Implications of Financial and Production Networks, the $(EC)^2$ Annual Conference, the Econometric Society North American Winter Meetings, the Vienna Workshop on High Dimensional Time Series in Macroeconomics and Finance, and the FRB San Francisco Conference in Honor of James Hamilton. We are especially grateful to Turan Bali, Gorkem Bostanci, Christian Brownlees, Fabio Canova, Umut Gokcen, M. Furkan Karaca, Laura Kaufmann, Serena Ng, Han Ozsoylev, Minchul Shin, David Veredas, and Tanju Yorulmazer. Demirer and Yılmaz thank the Turkish Scientific and Technological Research Council (TUBITAK) for financial support through Grant No. 111K500. The usual disclaimer applies.

REFERENCES

Acemoglu, D., Carvalho, V. M., Ozdaglar, A., & Tahbaz-Salehi, A. (2012). The network origins of aggregate fluctuations. *Econometrica*, *80*(5), 1977–2016.

Acharya, V., Engle, R., & Richardson, M. (2012). Capital shortfall: A new approach to ranking and regulating systemic risks. *American Economic Review*, *102*, 59–64.

Acharya, V., Pedersen, L. H., Philippon, T., & Richardson, M. (2017). Measuring systemic risk. *Review of Financial Studies*, *30*(1), 2–47.

Acharya, V., & Yorulmazer, T. (2007). Too many to fail: An analysis of time-inconsistency in bank closure policies. *Journal of Financial Intermediation*, *16*, 1–31.

Adrian, T., & Brunnermeier, M. (2016). CoVaR. *American Economic Review*, *106*, 1705–1741.

Alizadeh, S., Brandt, M., & Diebold, F. (2002). Range-based estimation of stochastic volatility models. *Journal of Finance*, *57*(3), 1047–1091.

Allen, F., & Gale, D. (1994). Limited market participation and the volatility of asset prices. *American Economic Review*, *84*, 933–955.

Allen, F., & Gale, D. (2000). Financial contagion. *Journal of Political Economy*, *108*, 1–33.

Allen, L., Bali, T., & Tang, Y. (2012). Does systemic risk in the financial sector predict future economic downturns? *Review of Financial Studies*, *25*, 3000–3036.

Andersen, T., Bollerslev, T., Christoffersen, P., & Diebold, F. (2013). Financial risk measurement for financial risk management. In Harris, M., Constantinedes, G., & Stulz, R. (Eds.), *Handbook of the Economics of Finance*, Vol. *2*. Amsterdam, Netherlands: Elsevier, pp. 1127–1220.

Babus, A. (2016). The formation of financial networks. *RAND Journal of Economics*, *47*(2), 239–272.

Barigozzi, M., & Brownlees, C. (2013). *Nets: Network Estimation for Time Series*, (Barcelona GSE Working Paper 723). Barcelona, Spain: Graduate School of Economics.

Bianchi, D., Billio, M., Casarin, R., & Guidolin, M. (2015). Modeling contagion and systemic risk. (SYRTO Working Paper Series, No. 10).

Billio, M., Getmansky, M., Lo, A., & Pelizzon, L. (2012). Econometric measures of connectedness and systemic risk in the finance and insurance sectors. *Journal of Financial Economics*, *104*, 535–559.

Bonaldi, P., Hortacsu, A., & Kastl, J. (2015). *An empirical analysis of funding costs spillovers in the euro-zone with application to systemic risk*, (NBER Working Paper Series No. 21462). Cambridge, MA: National Bureau of Economic Research.

Brownlees, C., & Engle, R. (2015). SRISK: A conditional capital shortfall index for systemic risk measurement (Working paper): Pompeu Fabra University and New York University.

Cifuentes, R., Ferrucci, G., & Shin, H. (2005). Liquidity risk and contagion. *Journal of the European Economic Association*, *3*, 556–566.

Diebold, F., & Yilmaz, K. (2009). Measuring financial asset return and volatility spillovers, with application to global equity markets. *Economic Journal*, *119*, 158–171.

Diebold, F., & Yilmaz, K. (2012). Better to give than to receive: Predictive measurement of volatility spillovers (with discussion). *International Journal of Forecasting*, *28*, 57–66.

Diebold, F., & Yilmaz, K. (2014). On the network topology of variance decompositions: Measuring the connectedness of financial firms. *Journal of Econometrics*, *182*, 119–134.

Easley, D., & Kleinberg, J. (2010). *Networks, crowds and markets*. Cambridge, UK: Cambridge University Press.

Garman, M. B., & Klass, M. J. (1980). On the estimation of security price volatilities from historical data. *Journal of Business*, *53*(1), 67–78.

Giglio, S., Kelly, B., & Pruitt, S. (2016). Systemic risk and the macroeconomy: An empirical evaluation. *Journal of Financial Economics*, *119*, 457–471.

Gorton, G. B. (2015). *The Maze of Banking: History, Theory, Crisis*. Oxford, UK: Oxford University Press.

Jackson, M. (2008). *Social and Economic Networks*. Princeton, NJ: Princeton University Press.

Jacomy, M., Heymann, S., Venturini, T., & Bastian, M. (2014). ForceAtlas2, a continuous graph layout algorithm for handy network visualization designed for the gephi software. *PLOS ONE*, *9*(6), e98679.

Koop, G., Pesaran, M., & Potter, S. (1996). Impulse response analysis in nonlinear multivariate models. *Journal of Econometrics*, *74*(1), 119–147.

Parkinson, M. (1980). The extreme value method for estimating the variance of the rate of return. *Journal of Business*, *53*(1), 61–65.

Pesaran, H., & Shin, Y. (1998). Generalized impulse response analysis in linear multivariate models. *Economics Letters*, *58*(1), 17–29.

Shleifer, A., & Vishny, R. (1992). Liquidity values and debt capacity: A market equilibrium approach. *Journal of Finance*, *47*, 1343–1366.

Tibshirani, R. (1996). Regression shrinkage and selection via the lasso. *Journal of the Royal Statistical Society, Series B*, *58*, 267–288.

Zou, H., & Zhang, H. (2009). On the adaptive elastic net with a diverging number of parameters. *Annals of Statistics*, *37*(4), 1733–1751.

SUPPORTING INFORMATION

Additional Supporting Information may be found online in the supporting information tab for this article.

How to cite this article: Demirer M, Diebold FX, Liu L, Yilmaz K. Estimating global bank network connectedness. *J Appl Econ*. 2018;33:1–15. https://doi.org/10.1002/jae.2585